



## Detecting Lysozyme Unfolding via the Fluorescence of Lysozyme Encapsulated Gold Nanoclusters

Nora Alkudaisi<sup>a</sup>, Ben A. Russell<sup>a</sup>, Barbara Jachimska<sup>b</sup> David J. S. Birch<sup>a</sup> and Yu Chen<sup>a†</sup>

Received 00th January 20xx,  
Accepted 00th January 20xx

DOI: 10.1039/x0xx00000x

www.rsc.org/

Protein misfolding plays a critical role in the formation of Amyloidosis type disease. Therefore, understanding and ability to track protein unfolding in a dynamic manner is of considerable interest. Fluorescence-based techniques are powerful tools for gaining real-time information about the local environmental conditions of a probe on the nanoscale. Fluorescent gold nanoclusters (AuNCs) are a new type of fluorescent probes which are <2 nm in diameter, incredibly robust and offer highly sensitive, wavelength tuneable emission. Their small size minimises intrusion and makes AuNCs ideal for studying protein dynamics. Lysozyme has previously been used to encapsulate AuNCs. The unfolding dynamics of Lysozyme under different environmental conditions have been well-studied and being an Amyloid type protein, makes Lysozyme an ideal candidate for encapsulating AuNCs in order to test their sensitivity to protein unfolding. In this study, we tracked the fluorescence characteristics of AuNCs encapsulated in Lysozyme while inducing protein unfolding by Urea, Sodium Dodecyl Sulphate (SDS) and elevated temperature and compared them to complimentary Circular Dichroism spectra. It is found that AuNC fluorescence emission is quenched upon induced protein unfolding either due to a decrease in Forster Resonance Energy Transfer (FRET) efficiency between tryptophan and AuNCs or solvent exposure of the AuNC. Fluorescence lifetime measurements confirmed quenching to be collisional via oxygen dissolved in a solution; increasing as the AuNC was exposed to the solvent during unfolding. Moreover, the longer decay component  $\tau_1$  was observed to decrease as the protein unfolded, due to the increased collisional quenching. It is suggested that AuNC sensitivity to solvent exposure might be utilised in the future as a new approach to studying and possibly even detecting Amyloidosis type diseases.

### Introduction

Protein function is highly dependent on protein tertiary structure and is crucial for the correct cellular function in all living things<sup>1–4</sup>. As such, any changes to protein tertiary structure can result in catastrophic cell loss and disease<sup>5–7</sup>. Neurodegenerative diseases such as Alzheimer's and Parkinson's have received much attention due to their debilitating nature and increasing number of patients; with a large focus on understanding how these diseases arise<sup>8</sup>. One major theory, which has seen many studies, describes these diseases as a result of the formation of protein aggregate fibrils formed by misfolded protein<sup>9–12</sup>. This aggregation is commonly referred to as Amyloidosis. The protein can be deposited in any tissue and organ, frequently affecting not only the brain but the heart, kidneys, liver and digestive tract which can result in organ failure<sup>13</sup>. Therefore, understanding the fundamental mechanism of protein misfolding and aggregation is vital to understanding the causes and develop

therapeutics for these diseases<sup>14</sup>. Previous studies of amyloidosis have involved different methods of inducing the destabilization of a protein's structure via altering pH<sup>15</sup>, solvent<sup>16</sup>, temperature<sup>17</sup> and the addition of Sodium Dodecyl Sulphate (SDS)<sup>18</sup> or Urea<sup>19</sup>. SDS is an anionic surfactant consisting of a 12-carbon tail connecting to a sulphate group, often used as a detergent. The negatively charged head typically forms bonds with amino acid residues with the positively charged side chains within proteins, such as Lysine, Arginine and Histamine, causing proteins to unfold<sup>20</sup>. Urea is also commonly used to study the unfolding dynamics of proteins<sup>21,22</sup>. Urea consists of two amide groups joined by a carbonyl functional group<sup>23</sup>. There are two mechanisms under which Urea can act as a denaturant of proteins. Firstly, the Urea can directly bind with the protein via electrostatic or nonpolar interactions; altering the structure of the protein and inducing unfolding and secondly, via an indirect mechanism where the Urea molecules destroy protein hydrophobic structures, thereby allowing water to penetrate into the protein centre<sup>24</sup>. Lysozyme (from chicken egg whites) is most commonly used as an ideal protein for studying amyloids due to its amyloidogenic properties and its similarity to human lysozyme<sup>25</sup>. Previously Lysozyme unfolding studies have been carried out using a number of different techniques including; Circular Dichroism Spectroscopy<sup>26</sup>, Raman Spectroscopy<sup>27</sup>, X-ray Crystallography<sup>28</sup> and Molecular Dynamics Simulations<sup>24</sup>.

<sup>a</sup> Department of Physics, SUPA, University of Strathclyde, John Anderson Building, 107 Rottenrow, Glasgow G4 0NG, UK.

<sup>b</sup> Jerzy Haber Institute of Catalysis and Surface Chemistry, Polish Academy of Sciences, Niezapominajek 8, 30-239 Cracow, Poland

<sup>c</sup> † Corresponding author; E-mail address: y.chen@strath.ac.uk

Among these techniques, fluorescence spectroscopy has been shown to be an excellent method of studying the formation of amyloids via either an attached fluorescent probe<sup>29</sup> or intrinsic fluorescence<sup>10</sup>. The two most common fluorescent probes used for tracking the formation of amyloids are Thioflavin-T (ThT) and Congo red. The fluorescence emission intensity of ThT is highly enhanced when trapped between beta sheets which form at later stages of amyloid formation. The major disadvantage of ThT as a means of tracking amyloid formation is that during the early stages of proto-fibril formation there are no beta sheets yet formed and as a result, the ThT dye is unresponsive<sup>30</sup>. In addition, SDS has also been shown to enhance ThT fluorescence emission intensity; making it impossible to study SDS induced amyloid formation<sup>31</sup>. Congo red exhibits a red shift in its absorption spectrum when binding to amyloids, however, this is also true when binding to smaller oligomers, making it difficult to track the early stages of amyloid fibril formation<sup>29</sup>. Congo red also exhibits a colour change at low pH making it unsuitable as a method of studying the amyloid formation and protein unfolding in acidic conditions<sup>32</sup>. Interestingly a new class of fluorophore – gold nanoclusters (AuNCs) encapsulated by Serum Albumin have received much interest recently<sup>33–36</sup> and have previously reported changes in fluorescence due to the encapsulating protein unfolding<sup>37–39</sup>. AuNCs have attracted interest due to their small size (less than 2 nm in diameter)<sup>40</sup>, luminescence in the near IR band<sup>41</sup>, large Stoke shift, long fluorescence lifetime<sup>42</sup>, biocompatibility<sup>43</sup> and water solubility<sup>44</sup>. Interestingly, Lysozyme is also capable of encapsulating gold nanoclusters<sup>45,46</sup> and as such, may be used as a means of probing lysozyme unfolding and amyloidosis. To this end, we studied how the fluorescence characteristics of AuNCs encapsulated by Lysozyme were affected during protein unfolding introduced via Urea, SDS and heating using steady-state, time-resolved fluorescence and Circular Dichroism spectroscopy.

## Materials and Methods

Lysozyme (crystallized and lyophilized powder, from chicken egg white) ( $\geq 90$  % purity), gold(III) chloride hydrate ( $>49.0$  % trace metals basis), Urea (crystallized) ( $\geq 98$  % purity), SDS (powder) (98 % purity), and Phosphate buffered saline (PBS) buffer were purchased from Sigma Aldrich and used without further purification. A stock solution of Lysozyme encapsulated AuNCs (Ly-AuNCs) was prepared using Wei's method<sup>47</sup>. Initially, a solution of lysozyme (5 mL, 10 mg/ml) was vigorously stirred with a solution of gold (5mL, 4 mM). After 2 minutes, an aqueous solution of NaOH (0.5 mL, 1M) was added to the Lysozyme/Au solution. The reaction was continuously stirred at 37 °C for 24 hours. Finally, the Ly-AuNC solution was dialysed into PBS buffer solution, using dialysis cassettes with a MWCO of 10,000 Da. All Ly-AuNC experiments were carried out with a 10 % diluted sample from stock (Lysozyme concentration of 33  $\mu$ M). Stock solutions of Urea were prepared in the concentration range of 1-8 M, dissolving the crystals in purified water at room temperature via stirring. A

stock solution of SDS was prepared at a concentration of 300 mM, dissolving the powder in purified water at room temperature via stirring. All fluorescence emission spectra were measured using a HORIBA Fluorolog 3. All fluorescence lifetimes were measured using the Time-Correlated Single Photon-Counting (TCSPC) technique on a HORIBA DeltaFlex. Excitation was carried out using a Delta Diode laser excitation source at 482 nm. Fluorescence lifetime decays were analysed using HORIBA DAS6 software. Circular Dichroism (CD) spectroscopy was carried out using a Jasco J-1500 spectrophotometer. For all measurements a quartz cell with 1mm path length was used in a nitrogen atmosphere. Each spectrum was taken from an average of 5 scans with a scan speed of 50 nm/min. All spectra were corrected for PBS buffer signals.

## Results and Discussion

### Effect of Urea on Ly-AuNCs Fluorescence

Previous studies have shown that to that 7.4 M of urea is sufficient to denature 50% of lysozyme<sup>48</sup>. The minimum required urea concentration to change the conformation of lysozyme is 8 M<sup>49</sup>. Lysozyme contains 6 fluorescent tryptophans in total. Four residues (62, 63, 108 and 111) are located in the helix-loop-helix domain and are solvent exposed. Residues 28 and 123 are located within the helix structure themselves and are buried within a hydrophobic pocket<sup>50</sup>. The microenvironment of these tryptophan residues is critical to understanding the changes in fluorescence and thus, the unfolding dynamics<sup>51</sup>. To understand the photophysics of Lysozyme unfolding via AuNC fluorescence, we increased the concentration of Urea in a solution of Ly-AuNCs in steps of 1 M and measured the changes to the Ly-AuNCs emission spectrum when exciting at 295 nm and 470 nm, as shown in Figure 1. From Figure 1 (A) we can see two peaks; the first peak centred on  $\sim 350$  nm is Tryptophan and a second larger fluorescence peak centred on  $\sim 700$  nm originating from the AuNCs.

To better understand the protein tertiary structure with increasing Urea, we observed the tryptophan peak fluorescence emission intensity and wavelength as a function of Urea concentration, as shown in Figure 2. The emission maximum can be seen to increase consistently (apart from a small dip at 6M) as a function of Urea concentration as well as a red shift of 4 nm in peak emission wavelength from 0-4 M of Urea and no further changes in the concentration range of 4-8 M of Urea; suggesting tryptophan is already water exposed during the partial unfolding between 0-4 M. This agrees with Kurtin *et. al.*, suggesting reduced quenching from neighbouring residues for the increase in fluorescence intensity and tryptophan becoming exposed to the polar water environment of the solution for the red shift in peak emission wavelength<sup>52</sup>. To illustrate the changes in fluorescence emission of AuNCs during Lysozyme unfolding, the peak emission intensity and wavelengths of AuNCs fluorescence as a function of Urea concentration in solution when excited at 295 and 470 nm

were shown in Figures 3 and 4. From Figure 3 it can be seen that the fluorescence emission intensity of AuNCs fluctuates when excited at 290 nm but decreases linearly when excited at 470 nm as a function of Urea concentration in solution.

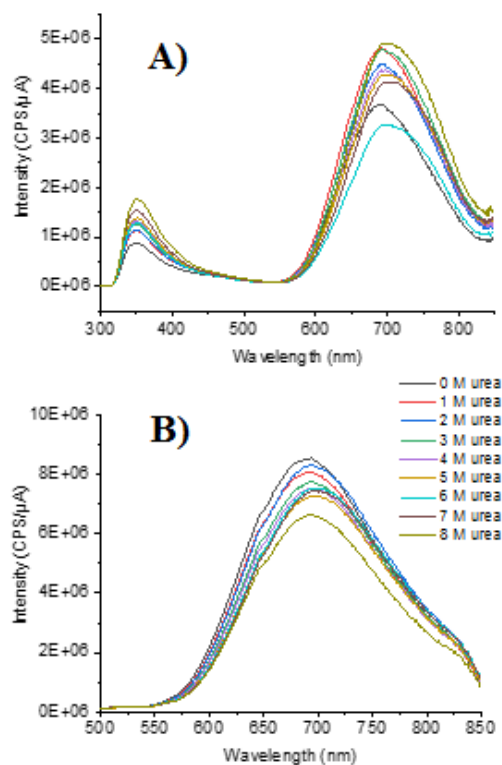


Figure 1. Fluorescence emission spectrum of Ly-AuNCs with increasing concentration of Urea added to solution, A) excitation 295 nm; B) excitation 470 nm.

The emission intensity decrease observed as the protein unfolds when excited at 470 nm is most likely due to increased collisional quenching of the AuNC as it becomes more exposed to the surrounding solvent<sup>37</sup>.

The minimal change in emission intensity, when excited at 295 nm, implies that while increasing collisional quenching and decreasing FRET efficiency as a result of a possible increase in the separation between tryptophan and AuNC as the Lysozyme unfold result in a decrease in emission, another effect modifies the emission of AuNC. Figure 4 shows that the AuNC maximum emission wavelength red shifts as the urea concentration increases. The red shift of AuNC emission and decrease in intensity was also reported in solvent-exposed gold nanoclusters encapsulated in different protein than Lysozyme<sup>38</sup>. However, an apparent difference in the redshift across the Urea concentration range was observed when excited at 295 nm and 470 nm, 16 nm vs. 4 nm, suggesting that different excitation routes lead to different inter-system crossing pathways. In addition to conformational effects, the changes in AuNC characteristics may also arise due to the interactions between Urea and Cysteine residues. Previously it has been shown that Urea preferentially binds to Cysteine

residues (30, 80 and 94) leading to changes in the structure at the disulphide bonds present in Lysozyme<sup>24,48</sup>. It is well known that sulphur-gold bonds are present within all protein encapsulated AuNCs, measured via XPS; acting as a critical stabilizing agent which is needed to form clusters within the protein<sup>45,53,54</sup>. Therefore, it is reasonable to assume that Urea may modify the binding of AuNC to protein, altering the fluorescence characteristics in the process. Further study is needed to disclose the mechanism.

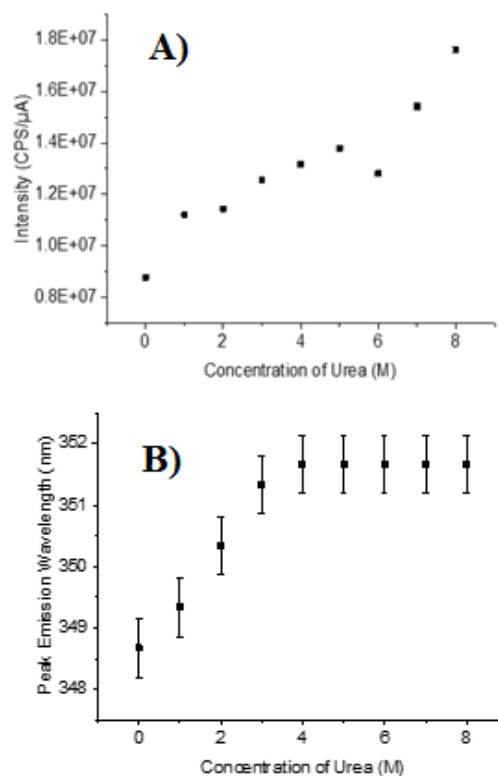


Figure 2 A) Fluorescence emission maximum intensity of native tryptophan emission from Ly-AuNCs, B) Fluorescence emission maximum wavelength; both as a function of increasing Urea concentration in solution. Excitation 295 nm.

To further explore the emission characteristics of AuNC emission during protein unfolding, the fluorescence lifetimes of AuNCs as a function of Urea concentration were measured. Fluorescence lifetimes were collected using a 482 nm pulsed light source over a measurable time of 13  $\mu$ s. The resulting fluorescence decay curves were analysed using a 3-exponential model. The results of the analysis are shown in Table 1. The three exponential model is shown to be a good fit to the fluorescence decay curve using the least squares method of goodness of fit analysis with a  $\chi^2$  value between 1.00-1.13 for all the data. The two major lifetime components of  $\sim$  2000 ns and  $\sim$  700 ns compare well with previously reported lifetime values for protein encapsulated AuNCs<sup>37,55,56</sup>. The shorter lifetime component is probably the result of scattered light from the sample.

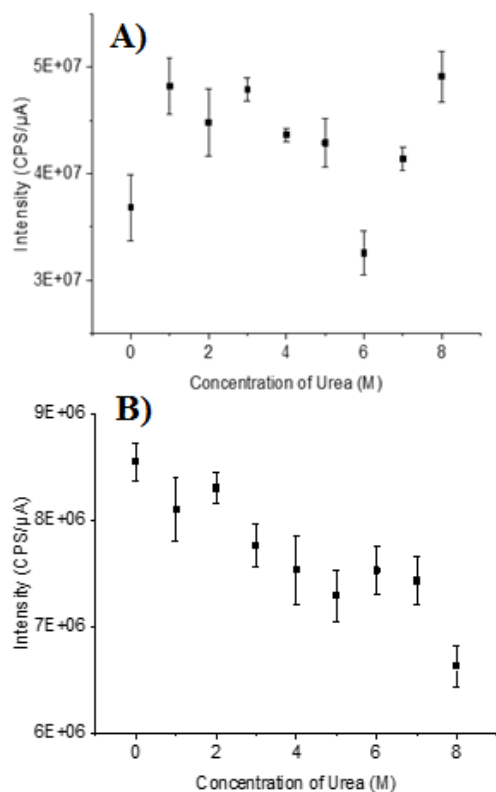


Figure 3. Fluorescence emission maximum intensity of AuNC emission from Ly-AuNCs, as a function of increasing Urea concentration in solution; A) excitation 295 nm, B) excitation 470 nm.

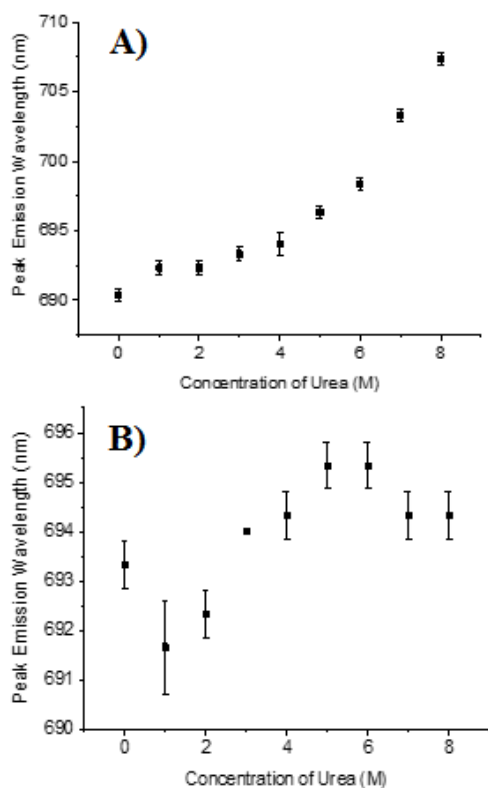


Figure 4. Fluorescence emission maximum wavelength of AuNC emission from Ly-AuNCs, as a function of increasing Urea concentration in solution; A) excitation 295 nm, B) excitation 470 nm.

From Table 1, we can see a clear decrease in the longer lifetime value  $\tau_1$  of  $2264 \pm 6$  ns at 0 M of Urea to  $1922 \pm 8$  ns at 8 M of Urea, whereas the decrease in the second shorter lifetime  $\tau_2$  is much smaller. This decrease in lifetime for  $\tau_1$  suggests that as the protein unfolds, the AuNC undergoes increased collisional quenching due to increased solvent exposure. To show the effect of added Urea in solution with Ly-AuNCs on the encapsulating protein's structure, CD spectroscopy was carried out on Ly-AuNCs with increasing Urea concentration shown in Figure 5.

Table 1. Fluorescence Lifetimes of AuNC emission with amplitudes with different concentrations of Urea added. Excitation 482

Conc. of urea (M)	$\tau_1$ [ns] (b <sub>1</sub> )	$\tau_2$ (ns) (b <sub>2</sub> )	$\tau_3$ (ns) (b <sub>3</sub> )	$\chi^2$
0	$2264 \pm 6$ (71.17 %)	$795 \pm 17$ (25.42 %)	$121 \pm 3$ (3.41 %)	1.09
1	$2136 \pm 5$ (73.04 %)	$728 \pm 15$ (23.72 %)	$109 \pm 3$ (3.25 %)	1.05
2	$2091 \pm 5$ (73.26 %)	$706 \pm 17$ (23.48 %)	$102 \pm 3$ (3.26 %)	1.12
3	$2168 \pm 6$ (71.13 %)	$760 \pm 17$ (25.01 %)	$119 \pm 3$ (3.85 %)	1.08
4	$2045 \pm 6$ (72.73 %)	$717 \pm 19$ (23.59 %)	$110 \pm 3$ (3.68 %)	1.09
5	$2016 \pm 5$ (72.74 %)	$697 \pm 16$ (23.99 %)	$97 \pm 3$ (3.27 %)	1.11
6	$2014 \pm 6$ (71.81 %)	$720 \pm 17$ (24.6 %)	$106 \pm 3$ (3.59 %)	1.10
7	$1975 \pm 5$ (72.96 %)	$679 \pm 15$ (23.77 %)	$92 \pm 3$ (3.26 %)	1.13
8	$1922 \pm 8$ (75.52 %)	$617 \pm 26$ (21.62 %)	$89 \pm 5$ (2.86 %)	1.08

From Figure 5 (A) we can see that the CD spectrum of Lysozyme shifts to shorter wavelengths after synthesis of encapsulated AuNCs from a trough at 208 nm, a feature due to the alpha helix content of Lysozyme, to a smaller trough at 204 nm, indicating a loss of alpha helicity to a more disordered conformation. Upon increasing the Urea concentration in solution with Ly-AuNCs we observe that the spectral trough position does not change but decreases slightly in magnitude, as seen in Figure 5 (B). This small decrease in magnitude is attributed to the Urea having a small effect on the Ly-AuNCs conformation, resulting in further loss of native structure. From this study, we can ascertain that the AuNC fluorescence of Ly-AuNCs is sensitive to the partial conformational changes induced via Urea despite the impact of Urea on the structure of Ly-AuNCs being small. The Urea binding may be partially responsible for changes to the AuNC emission, especially in the case of 295 nm excitation due to conformational changes increasing the separation between Trp and AuNCs resulting in a decrease in the FRET efficiency between the two fluorophores.

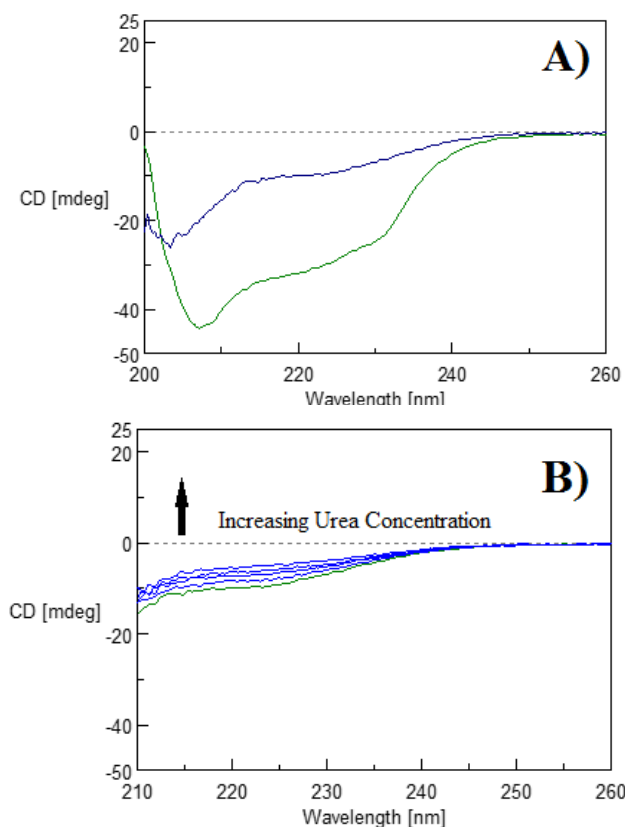


Figure 5. CD spectra of: A) Lysozyme (green) and Ly-AuNCs (Blue). B) Ly-AuNC with increasing Urea concentration. All CD spectra were recorded in PBS buffer solution at pH 7.4.

### Effect of SDS on Ly-AuNC Fluorescence

The influence of SDS induced lysozyme unfolding on the fluorescence characteristics of AuNCs was also studied in a similar fashion to Urea. SDS was added to a solution of Ly-AuNCs at concentrations between 0–9 mM and fluorescence spectra were measured at both 295 nm and 470 nm excitation. The fluorescence spectra of Ly-AuNCs with different concentrations of SDS added are shown in Figure 6. From Figure 6 (A) we again see the characteristic 2 peak fluorescence emission spectra of Ly-AuNCs when excited at 295 nm, with the first peak originating from Tryptophan and the second from AuNCs. Figure 6 (B) shows the fluorescence emission spectra of Ly-AuNCs when the AuNC is directly excited at 470 nm. Interestingly, in both spectra, the peak maximum wavelength of AuNCs does not shift upon adding SDS, however, a small blue shift of 2 nm was observed for the peak emission wavelength of tryptophan. This 2 nm blue shift agrees well with Sun *et al.* who also observed a 2 nm blue shift for tryptophan emission when Lysozyme and SDS were in solution with the same ratio of SDS to Lysozyme<sup>20</sup>. At this SDS/Lysozyme ratio, the same group reported a decrease in alpha helix content of the protein. This suggests that the SDS does cause a change to the protein conformation at these concentrations but does not alter the binding of AuNC to protein as Urea does and that surface tryptophan becomes buried within the hydrophobic structure.

To better display the effect of SDS on the fluorescence intensity of tryptophan and AuNCs the maximum fluorescence intensity of both were plotted as a function of SDS concentration, as shown in Figure 7 and 8. From Figure 7 we can see that the maximum fluorescence intensity of native tryptophan initially increases before levelling off as a function of SDS concentration. Between 0–3 mM of SDS concentration in solution, the fluorescence maximum of native tryptophan fluorescence rises linearly with SDS concentration.

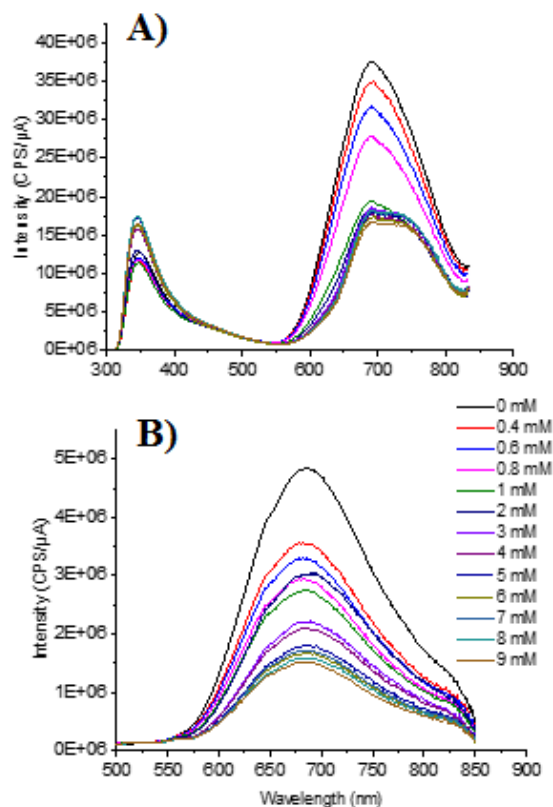


Figure 6. Fluorescence emission spectrum of Ly-AuNCs with increasing concentration of SDS added to solution, (A) excitation 295 nm; (B) excitation 470 nm.

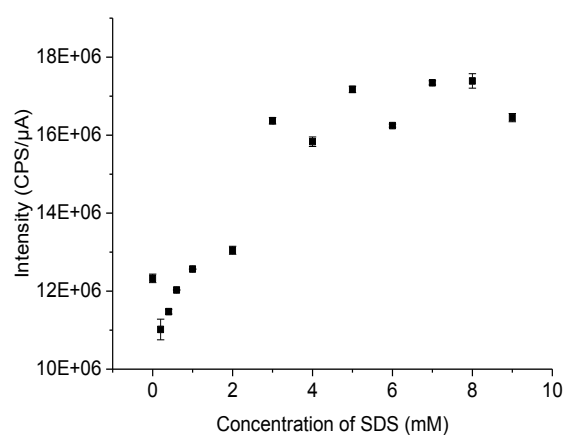


Figure 7. Fluorescence emission maximum intensity of native tryptophan emission from Ly-AuNCs, as a function of increasing SDS concentration in solution. Excitation 295 nm.

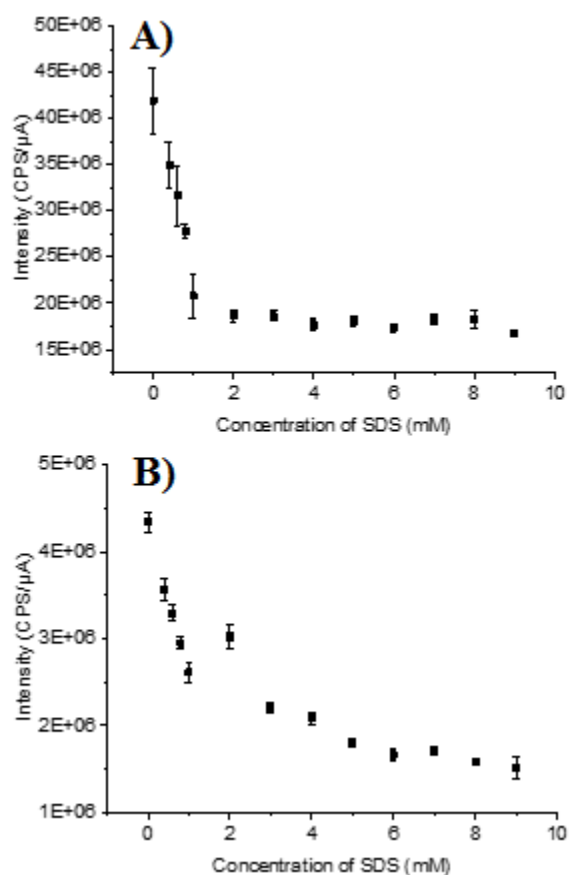


Figure 8. Fluorescence emission maximum intensity of AuNC emission from Ly-AuNCs, as a function of increasing SDS concentration in solution; A) excitation 295 nm, B) excitation 470 nm.

This rise could be due to the fact that tryptophan is less exposed to water resulting from the protein conformational change introduced by SDS binding to Lysozyme<sup>57</sup>. It is also possible that this increase arises from a reduced energy transfer due to an increase in tryptophan/AuNC separation. From Figure 8 we can see that AuNC fluorescence emission maximum has a rapid linear decrease between 0-1 mM of SDS in solution and then a slower linear decrease between 1-9 mM of SDS in solution when exciting at both 295 nm and 470 nm. The same initially fast decrease for both excitations indicates that the decrease is not governed by a decrease in FRET efficiency due to increased tryptophan/AuNC separation, however, the magnitude of the fluorescence maximum intensity decrease is slightly larger when excited at 295 nm compared with 470 nm indicating the contribution from a reduced FRET. Due to the rapid decrease, it is most likely the protein undergoes major unfolding at the location of the AuNC between concentrations of 0-1 mM SDS; resulting in increasing collisional quenching of the AuNC in solution. Further increase in SDS doesn't cause a significant decrease in the AuNC emission intensity maximum, suggesting no major alteration to the local environment around AuNC.

In order to determine that the change in AuNCs emission is due to collisional quenching as Lysozyme unfolds rather than the interaction with SDS, we studied the fluorescence lifetimes of Ly-AuNCs, focussing on directly exciting the AuNC at different concentrations of SDS in solution. The results of this experiment are shown in Table 2. As in previous studies with Urea, we use a 3 exponential function to fit the measured fluorescence decay curves, with a  $\chi^2$  value between 1.05-1.15, indicating the data description is of good quality. Again, we find that only the longer decay time,  $\tau_1$ , is sensitive to the increasing SDS concentration in solution, with  $\tau_2$  fluctuating but remaining within error and  $\tau_3$  the scattering proportion of the fitted decay curve. The long fluorescence lifetime was seen to decrease by  $\sim 100$  ns over between 0-1 mM SDS in solution and then only a further 150 ns between 1-9 mM, indicating that collisional quenching is taking place and that the biggest local environmental change due to unfolding happens within the 0-1 mM SDS concentration range; agreeing well with the fluorescence emission spectra data from Figure 7. Due to the lack of red shift in the fluorescence peak emission wavelength for AuNCs excited at both 295 nm and 470 nm, the changes in fluorescence emission maximum and fluorescence decay time can be attributed to the effect of solvent exposure and increased collisional quenching as a result. To show the effect of added SDS in solution with Ly-AuNCs on the encapsulating protein's structure, CD spectroscopy was carried out on Ly-AuNCs with increasing SDS concentration as shown in Figure 9.

Table 2. Fluorescence Lifetimes of AuNC emission with amplitudes with different concentrations of SDS added. Excitation 482 nm.

Conc. of SDS (mM)	$\tau_1$ [ns] (B <sub>1</sub> )	$\tau_2$ [ns] (B <sub>2</sub> )	$\tau_3$ [ns] (B <sub>3</sub> )	$\chi^2$
0	2159 ± 8 (69.89%)	825 ± 28 (26.14%)	160 ± 5 (3.97%)	1.05
1	2049 ± 8 (69.46%)	755 ± 22 (27.11%)	125 ± 5 (3.43%)	1.10
2	2057 ± 10 (67.54%)	824 ± 31 (28.52%)	146 ± 5 (3.94%)	1.14
3	2037 ± 9 (68.24%)	802 ± 34 (27.76%)	148 ± 5 (4.01%)	1.11
4	2015 ± 9 (68.3%)	758 ± 26 (28.2%)	127 ± 5 (3.5%)	1.15
5	1979 ± 9 (68.07%)	757 ± 31 (27.79%)	140 ± 5 (4.14%)	1.14
6	1962 ± 8 (70.0%)	723 ± 23 (26.59%)	108 ± 4 (3.4%)	1.14
7	1973 ± 7 (72.33%)	714 ± 23 (24.72%)	114 ± 5 (2.95%)	1.09
8	2078 ± 10 (65.68%)	821 ± 32 (30.16%)	147 ± 5 (4.15%)	1.13
9	1909 ± 8 (68.06%)	742 ± 18 (27.73%)	143 ± 10 (4.21%)	1.14

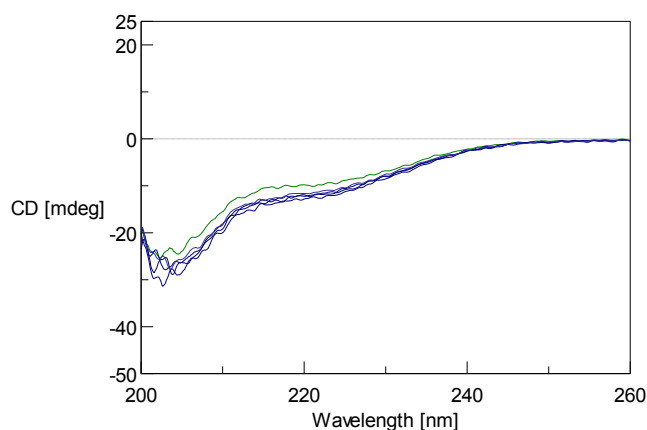


Figure 9. CD spectra of Ly-AuNCs with increasing SDS in solution. Ly-AuNC spectrum is shown in green, while Ly-AuNCs with SDS added are shown in blue. All measurements were taken in PBS buffer at pH 7.4.

From Figure 9 we can see that initially upon adding 2 mM of SDS to Ly-AuNCs in solution an increase in disordered structure is observed, upon further increasing the SDS concentration no clear further changes are observed in the Ly-AuNCs structure. The initial increase in the disordered structure feature seen as a trough at 203 nm further lends weight to the idea that the dramatic initial decrease in AuNC fluorescence observed results from a major unfolding of the encapsulating protein.

#### Effect of Elevated Temperature on Ly-AuNC Fluorescence

In order to remove any effects caused by interactions between protein and denaturants, temperature-based experiments were carried out to better understand the response of AuNC fluorescence to the unfolding and exposure of AuNC to the solvent. To this end, samples of Ly-AuNCs were heated and stabilised at 65 °C and the fluorescence emission of tryptophan and AuNCs were monitored over a period of 16 hours, exciting at 295 nm and 470 nm. This temperature was selected as Venkataramani *et al.* previously showed that Lysozyme begins to lose its tertiary structure at this temperature<sup>58</sup>. The fluorescence emission maximum of tryptophan as a function of time spent at 65 °C is shown in Figure 10. Interestingly tryptophan emission decreases in two steps, similar to the AuNC decrease as seen in Figure 8. The fast decrease in Trp emission in the first hour of heating indicates that the protein undergoes a major unfolding event resulting in tryptophan becoming solvent exposed and undergoes increased collisional quenching. The peak emission wavelength was also red shifted during this time by 4 nm and then remained unchanged for the duration of the experiment. From 1-16 hours the fluorescence maximum emission intensity continues to decrease linearly but at a slow rate, indicating the protein undergoes further unfolding; exposing the tryptophan to higher rates of collisional quenching. The fluorescence emission maximum of AuNCs was also recorded during heating, exciting at 295 nm and 470 nm. The results are displayed in Figure 11.

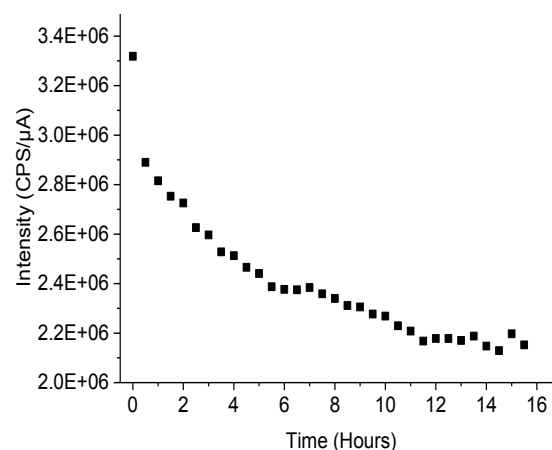


Figure 10. Fluorescence emission maximum intensity of native tryptophan emission from Ly-AuNCs, as a function of time spent at 65 °C. Excitation 295 nm.

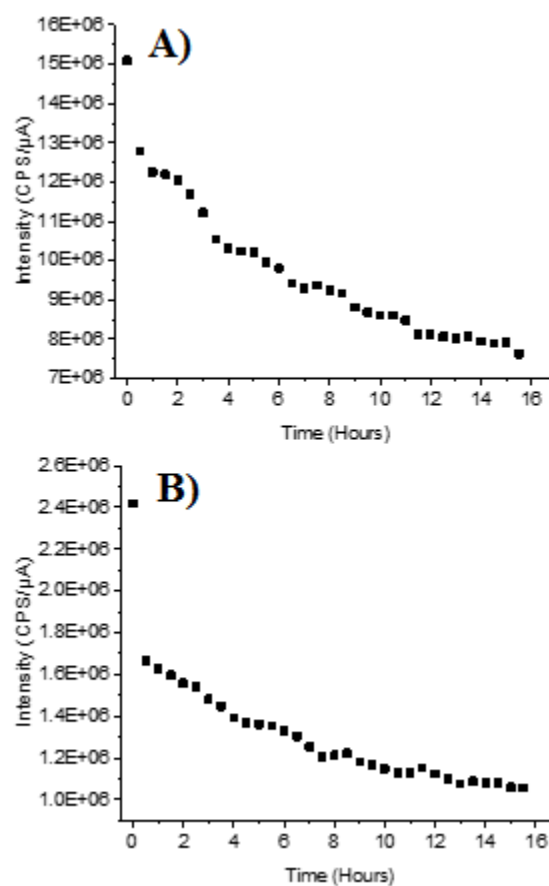


Figure 11. Fluorescence emission maximum intensity of AuNC emission from Ly-AuNCs, as a function of time spent at 65 °C; A) excitation 295 nm, B) excitation 470 nm.

### Effect of Oxygen in Solution on Ly-AuNC Fluorescence

In solution, Oxygen is well known to act as a collisional quencher of numerous fluorescent molecules and dyes<sup>59–61</sup> due to its triplet ground state inducing intersystem crossing. To confirm the effect of collisional quenching on the fluorescence characteristics of Ly-AuNCs, oxygen was removed by bubbling nitrogen into the Ly-AuNCs solution, a commonly used technique for the removal of dissolved oxygen in water<sup>62</sup>. Nitrogen gas was bubbled through the solution of Ly-AuNCs for 20 minutes and fluorescence spectra and fluorescence lifetime measurements were immediately carried out, as shown in Figure 12 and Table 3.

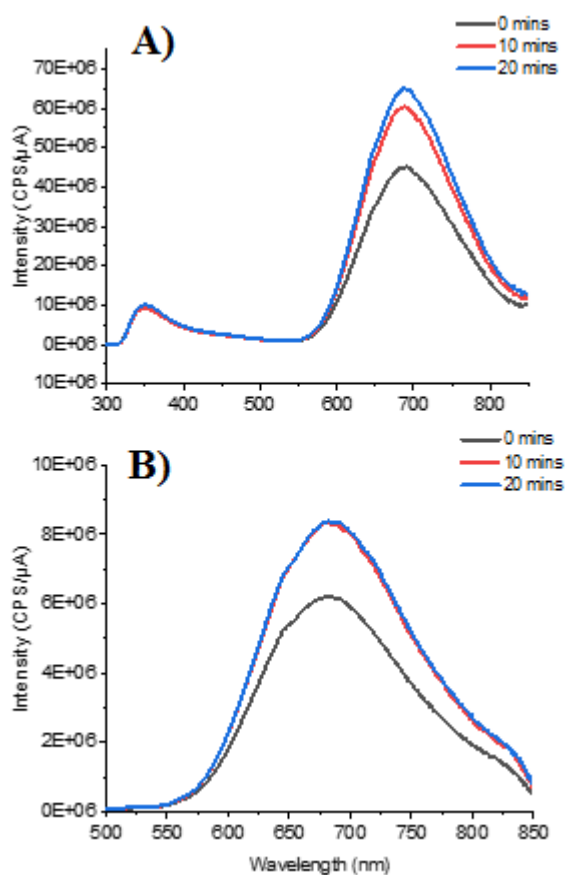


Figure 12. Fluorescence emission spectrum of Ly-AuNCs in the presence and absence of dissolved oxygen in solution, (A) excitation 295 nm; (B) excitation 470 nm.

Table 3. Fluorescence Lifetimes of AuNC emission with amplitudes in the presence and absence of dissolved oxygen in solution. Excitation 482 nm.

	$\tau_1$ (ns) (B <sub>1</sub> )	$\tau_2$ (ns) (B <sub>2</sub> )	$\tau_3$ (ns) (B <sub>3</sub> )	$\chi^2$
Present	2357 ± 20 (33.97 %)	1021 ± 45 (25.56 %)	199 ± 7 (40.57 %)	1.07
Not present	2647 ± 25 (32.67 %)	1100 ± 43 (26.40 %)	184 ± 7 (40.93 %)	1.10

From Figure 12 it is clear that while tryptophan emission is not affected by the removal of oxygen possibly due to FRET with AuNCs and its faster decay time, the AuNCs themselves have a large increase in the fluorescence emission intensity due to a reduced non-radiative relaxation from oxygen collisional quenching. When exciting at 470 nm the same effect can be seen. As previous, a 3 exponential fitting was used to fit the fluorescence decay curve and no change of  $\tau_3$  was found as might be expected for scattered light. An increase in fluorescence decay time indicates that collisional quenching has been reduced upon the removal of dissolved oxygen, resulting in the AuNC remaining in the excited state for a longer period of time on average.

### Conclusions

The sensitivity of AuNCs to Lysozyme unfolding induced via Urea, SDS and elevated temperature have been elucidated via steady-state, time-resolved fluorescence and Circular Dichroism spectroscopy. It was found that in all three cases the major factor of reduced fluorescence emission was due to the exposure of the AuNC to the surrounding solvent and subsequent collisional quenching by dissolved oxygen. In the case of Urea and SDS induced quenching, tryptophan emission was initially recorded to increase, however, the mechanism is believed to be different; for Urea the observed increase was attributed to reduced quenching and FRET from neighbouring residues, while for SDS the tryptophan becomes less solvent exposed and thus collisional quenching decreases. In the case of SDS and elevated temperature, an initial fast linear decrease of AuNC maximum fluorescence intensity was observed followed by a long, slow linear decrease. For SDS it was seen that the CD spectra rapidly changes upon initial addition of SDS, with subsequent increases in SDS concentration having less of an effect on protein structure. We believe that the initial fast decrease is due to a rapid change in the protein structure at the location of the AuNCs, resulting in solvent exposure, followed by a further unfolding of the protein which did not significantly affect the AuNC location in terms of further solvent exposure. The fluorescence decay components of AuNCs, when excited at 482 nm, were found to be partly sensitive to protein unfolding. The longer decay component  $\tau_1$  was observed to decrease as the protein unfolded, due to the increased collisional quenching. The shorter decay component  $\tau_2$  was found to be less if at all sensitive to the protein unfolding. Oxygen removal studies found that AuNC fluorescence emission is highly sensitive to dissolved oxygen in solution. Therefore oxygen is the most likely reason for quenching upon protein unfolding. This study highlights the possibility of using AuNCs as a useful probe for protein unfolding studies. It is envisaged that further study on the location of AuNC within each protein would shine a light on employing AuNCs to study protein unfolding dynamics.

## Conflicts of interest

There are no conflicts to declare.

## Acknowledgements

Nora Alkudaisi acknowledges a PhD Studentship from the Saudi Arabian Cultural Bureau.

## References

- 1 C. A. Orengo, A. E. Todd and J. M. Thornton, *Curr. Opin. Struct. Biol.*, 1999, **9**, 374–382.
- 2 C. Zhang and S.-H. Kim, *Curr. Opin. Chem. Biol.*, 2003, **7**, 28–32.
- 3 T. R. Hvidsten, A. Lægread, A. Kryshafovych, G. Andersson, K. Fidelis and J. Komorowski, *PLoS One*, 2009, **4**, e6266.
- 4 H. Hegyi and M. Gerstein, *J. Mol. Biol.*, 1999, **288**, 147–164.
- 5 T. K. Chaudhuri and S. Paul, *FEBS J.*, 2006, **273**, 1331–1349.
- 6 J. S. Valastyan and S. Lindquist, *Dis. Model. Mech.*, 2014, **7**, 9–14.
- 7 T. Nakamura and S. A. Lipton, *Apoptosis*, 2009, **14**, 455–468.
- 8 P. Sweeney, H. Park, M. Baumann, J. Dunlop, J. Frydman, R. Kopito, A. McCampbell, G. Leblanc, A. Venkateswaran, A. Nurmi and R. Hodgson, *Transl. Neurodegener.*, 2017, **6**, 1–13.
- 9 C. M. Dobson, *Philos. Trans. R. Soc. Lond. B. Biol. Sci.*, 2001, **356**, 133–45.
- 10 O. J. Rolinski, T. Wellbrock, D. J. S. Birch and V. Vysheirsky, *J. Phys. Chem. Lett.*, 2015, **6**, 3116–3120.
- 11 J. Nasica-Labouze, P. H. Nguyen, F. Sterpone, O. Berthoumieu, N.-V. Buchete, S. Coté, A. De Simone, A. J. Doig, P. Faller, A. Garcia, A. Laio, M. S. Li, S. Melchionna, N. Mousseau, Y. Mu, A. Paravastu, S. Pasquali, D. J. Rosenman, B. Strodel, B. Tarus, J. H. Viles, T. Zhang, C. Wang and P. Derreumaux, *Chem. Rev.*, 2015, **115**, 3518–3563.
- 12 A. M. Streets, Y. Sourigues, R. R. Kopito, R. Melki and S. R. Quake, *PLoS One*, 2013, **8**, 1–10.
- 13 A. D. Wechalekar, J. D. Gillmore and P. N. Hawkins, *Lancet*, 2016, **387**, 2641–2654.
- 14 T. Scheibel and J. Buchner, in *Molecular Chaperones in Health and Disease*, eds. K. Starke and M. Gaestel, Springer Berlin Heidelberg, Berlin, Heidelberg, 2006, pp. 199–219.
- 15 V. K. Ravi, T. Swain, N. Chandra and R. Swaminathan, *PLoS One*, DOI:10.1371/journal.pone.0087256.
- 16 A. Cao, D. Hu and L. Lai, *Protein Sci.*, 2004, **13**, 319–324.
- 17 M. R. Krebs, D. K. Wilkins, E. W. Chung, M. C. Pitkeathly, A. K. Chamberlain, J. Zurdo, C. V. Robinson and C. M. Dobson, *J. Mol. Biol.*, 2000, **300**, 541–9.
- 18 J. M. Khan, A. Qadeer, S. K. Chaturvedi, E. Ahmad, S. A. Rehman, S. Gourinath and R. H. Khan, *PLoS One*, DOI:10.1371/journal.pone.0029694.
- 19 S. S. Wang, Y. T. Hung, P. Wang and J. W. Wu, *Korean J. Chem. Eng.*, 2007, **24**, 787–795.
- 20 Y. Sun, P. L. O. Filho, J. C. Bozelli, J. Carvalho, S. Schreier and C. L. P. Oliveira, *Soft Matter*, 2015, **11**, 7769–7777.
- 21 R. Kumaran and P. Ramamurthy, *J. Fluoresc.*, 2011, **21**, 1499–1508.
- 22 N. Shimaki, K. Ikeda and K. Hamaguchi, 1971, **70**, 497–508.
- 23 C. Higgins, 2016, 1–6.
- 24 M. Gao, Z. She and R. Zhou, *J. Phys. Chem. B*, 2010, **114**, 15687–15693.
- 25 R. Swaminathan, V. K. Ravi, S. Kumar, M. V. S. Kumar and N. Chandra, *Adv. Protein Chem. Struct. Biol.*, 2011, **84**, 63–111.
- 26 K. P. Barnes, J. a Gordon and J. R. Warren, *J. Biol. Chem.*, 1972, **247**, 1708–.
- 27 A. Hédoux, S. Krenzlin, L. Paccou, Y. Guinet, M.-P. Flament and J. Siepmann, *Phys. Chem. Chem. Phys.*, 2010, **12**, 13189.
- 28 T. Raskar, S. Khavnekar and M. Hosur, *Sci. Rep.*, 2016, **6**, 32277.
- 29 I. Maezawa, H. S. Hong, R. Liu, C. Y. Wu, R. H. Cheng, M. P. Kung, H. F. Kung, K. S. Lam, S. Oddo, F. M. LaFerla and L. W. Jin, *J. Neurochem.*, 2008, **104**, 457–468.
- 30 S. Kumar, A. K. Singh, G. Krishnamoorthy and R. Swaminathan, *J. Fluoresc.*, 2008, **18**, 1199–1205.
- 31 S. Kumar, V. K. Ravi and R. Swaminathan, *Biochem. J.*, 2008, **415**, 275–288.
- 32 J. M. Khan, S. K. Chaturvedi, S. K. Rahman, M. Ishtikhar, A. Qadeer, E. Ahmad and R. H. Khan, *Soft Matter*, 2014, **10**, 2591–9.
- 33 B. A. Russell, P. A. Mulheran, D. J. S. Birch and Y. Chen, *Phys. Chem. Chem. Phys.*, 2016, **18**, 22874–22878.
- 34 L. Shang and G. U. Nienhaus, *Biophys. Rev.*, 2012, **4**, 313–322.
- 35 D. M. Chevrier, A. Chatt and P. Zhang, *J. Nanophotonics*, 2012, **6**, 1–16.
- 36 B. A. Russell, B. Jachimska, I. Kralka, P. A. Mulheran and Y. Chen, *J. Mater. Chem. B*, 2016, **4**, 6876–6882.
- 37 B. A. Russell, K. Kubiak-Ossowska, P. A. Mulheran, D. J. S. Birch and Y. Chen, *Phys. Chem. Chem. Phys.*, 2015, **17**, 21935–21941.
- 38 R. Chib, S. Butler, S. Raut, S. Shah, J. Borejdo, Z. Gryczynski and I. Gryczynski, *J. Lumin.*, 2015, **168**, LUMIND1500227.
- 39 X.-L. L. Cao, H.-W. W. Li, Y. Yue and Y. Wu, *Vib. Spectrosc.*, 2013, **65**, 186–192.
- 40 R. Jin, *Nanoscale*, 2010, **2**, 343–362.
- 41 J. Xie, Y. Zheng and J. Y. Ying, *J. Am. Chem. Soc.*, 2009, **131**, 888–889.
- 42 S. Raut, R. Chib, S. Butler, J. Borejdo, Z. Gryczynski and I. Gryczynski, *Methods Appl. Fluoresc.*, 2014, **2**, 35004.
- 43 K. Zheng, M. I. Setyawati, D. T. Leong and J. Xie, *ACS Nano*, 2017, **11**, 6904–6910.
- 44 W. Ding, Y. Liu, Y. Li, Q. Shi, H. Li, H. Xia, D. Wang and X. Tao, *RSC Adv.*, 2014, **4**, 22651.
- 45 Y. Xu, J. Sherwood, Y. Qin, D. Crowley, M. Bonizzoni and Y. Bao, *Nanoscale*, 2014, **6**, 1515–1524.
- 46 B. A. Russell, B. Jachimska, P. Komorek, P. A. Mulheran and Y. Chen, *Phys. Chem. Chem. Phys.*, DOI:10.1039/c7cp00540g.
- 47 H. Wei, Z. Wang, L. Yang, S. Tian, C. Hou and Y. Lu, *Analyst*,

- 2010, **135**, 1406–1410.
- 48 J. Y. Chang and L. Li, *FEBS Lett.*, 2002, **511**, 73–78.
- 49 A. C. Pike and K. R. Acharya, *Protein Sci.*, 1994, **3**, 706–10.
- 50 M. S. Weiss, G. J. Palm and R. Hilgenfeld, *Acta Crystallogr. Sect. D*, 2000, **56**, 952–958.
- 51 J. R. Lakowicz, *Principles of Fluorescence Spectroscopy*, Springer, Baltimore, 3rd edn., 2006.
- 52 W. E. Kurtin and J. M. Lee, *Biochem. Mol. Biol. Educ.*, 2002, **30**, 244–247.
- 53 X. Wen, P. Yu, Y. Toh and J. Tang, .
- 54 A. R. Garcia, I. Rahn, S. Johnson, R. Patel, J. Guo, J. Orbulescu, M. Micic, J. D. Whyte, P. Blackwelder and R. M. Leblanc, *Colloids Surf. B. Biointerfaces*, 2013, **105**, 167–72.
- 55 N. Alkudaisi, B. A. Russell, D. J. S. Birch and Y. Chen, *Submiss.*
- 56 S. Raut, R. Chib, R. Rich, D. Shumilov, Z. Gryczynski and I. Gryczynski, *Nanoscale*, 2013, **5**, 3441–3446.
- 57 P. R. Callis and T. Liu, *J. Phys. Chem. B*, 2004, **108**, 4248–4259.
- 58 S. Venkataramani, J. Truntzer and D. Coleman, *J. Pharm. Bioallied Sci.*, 2013, **5**, 148–153.
- 59 W. M. Vaughan and G. Weber, *Biochemistry*, 1970, **9**, 464–473.
- 60 J. R. Lakowicz and G. Weber, *Biochemistry*, 1973, **12**, 4161–4170.
- 61 D. Magde, R. Wong and P. G. Seybold, *Photochem. Photobiol.*, 2002, **75**, 327–34.
- 62 I. B. Butler, M. A. A. Schoonen and D. T. Rickard, *Talanta*, 1994, **41**, 211–215.